

Quantitative Assessment of 2-dimensional Parameters in Tomographic Images by Using Different Segmentation Methods

Rafael V. Camargo, DDS, MSc,*
 Jardel F. Mazzi-Chaves, DDS,
 MSc, PhD,*[†] Graziela B. Leoni,
 DDS, MSc, PhD,[‡]
 Karla F. Vasconcelos, DDS,
 MSc, PhD,[†] Alessandro Lamira,
 DDS, MSc, PhD,*
 Reinhilde Jacobs, DDS, MSc,
 PhD,^{‡§} and Manoel D. Sousa-
 Neto, DDS, MSc, PhD*

ABSTRACT

Introduction: The purpose of this study was to assess the accuracy of 2-dimensional morphometric parameters of root canals on different cone-beam computed tomographic (CBCT) images using 2 segmentation methods (operator dependent and Otsu's automatic), considering micro-computed tomographic (micro-CT) images as the reference standard.

Methods: Ten mandibular molars were scanned by micro-CT imaging and 3 different CBCT devices: Accuitomo (J Morita Corporation, Kyoto, Japan), NewTom 5G (CEFLA, Imola, Italy), and NewTom VGi evo (CEFLA). The images were standardized and recorded using MeVisLab software (MeVis Medical Solutions AG, Bremen, Germany). Two calibrated examiners assessed the images of axial reconstructions quantitatively by 2-dimensional parameters (area, perimeter, roundness, and largest and smallest diameter). Fleiss kappa was performed to check interrater and intrarater reliability. The absolute error was calculated as the means and standard deviation. One-way analysis of variance was performed for comparison between the methods used by the operator and Otsu's automatic thresholding. To determine the accuracy of CBCT devices, the absolute error rate of each parameter was calculated using micro-CT measurements as the reference value with thresholding determined by the operator.

Results: The thresholding method performed by the operator had lower absolute error values for area, perimeter, and major and minor diameters, differing ($P < .05$) from Otsu's automatic method, with no differences between the CBCT machines. **Conclusions:** An overestimation of area, roundness, and major and minor diameters and an underestimation of the perimeter were shown for the 3 CBCT machines evaluated. Thresholding determined by the operator is more accurate than that determined by Otsu's automatic method for the assessment of 2-dimensional morphometric parameters, which could direct influence in the diagnosis and endodontic treatment plan. (*J Endod* 2020; ■:1–6.)

KEY WORDS

Absolute error; cone beam computed tomography; microcomputed tomography; Otsu's thresholding

When combined with clinical and periapical radiographic examination, cone-beam computed tomographic (CBCT) images may aid in the diagnosis, treatment planning, image-guided treatment, and follow-up in endodontic therapy^{1–8}. Additionally, different software enables multiplanar evaluation to assess length, area, perimeter, and volume and provide essential data for diagnosis and endodontic planning^{5,9}. These evaluations may be performed by means of image segmentation, which consists of a technique that allows an objective measurement by delineating structures or regions of interest.

Nowadays, a few CBCT devices may reach the necessary image quality, spatial resolution, and accuracy to allow their application in clinical endodontics. However, the use of conventional segmentation methods (eg, fixed thresholding) to segment structures using CBCT images may be limited, mainly because of its relatively low-contrast resolution as well as the presence of different kind of artifacts.

Micro-computed tomographic (micro-CT) imaging has been used as the reference standard for *in vitro* assessment of root canal morphology, biomechanical preparation, and cleaning as well as for

SIGNIFICANCE

The indication of CBCT imaging for the assessment of area, perimeter, roundness, and major and minor diameters of root canals should be viewed with caution because these parameters had significant findings regarding overestimation and underestimation

From the *Department of Restorative Dentistry, School of Dentistry of Ribeirão Preto, University of São Paulo, São Paulo, Brazil; [†]OMFS IMPATH Research Group, Department of Imaging and Pathology, Faculty of Medicine, University of Leuven, University Hospitals Leuven, Leuven, Belgium; [‡]Faculty of Dentistry, University of Ribeirão Preto, Ribeirão Preto, Brazil; and [§]Department of Dental Medicine, Karolinska Institute, Stockholm, Sweden

Address requests for reprints to Dr Manoel D. Sousa-Neto, Department of Restorative Dentistry, School of Dentistry of Ribeirão Preto, University of São Paulo, Rua Célia de Oliveira Meirelles 350, 14024-070 Ribeirão Preto, SP, Brazil. E-mail address: sousanet@forp.usp.br 0099-2399/\$ - see front matter

Copyright © 2020 American Association of Endodontists.

<https://doi.org/10.1016/j.joen.2020.01.012>

obturation and endodontic retreatment protocols^{10–12}. This image modality allows for reliable microstructural analysis with high spatial resolution on a micrometric scale by means of thresholding of the region of interest^{13,14}. However, micro-CT imaging cannot be used in a clinical patient setting yet, considering the required scanning time and limited field of view.

Therefore, the aim of the present study was to assess the accuracy of 2-dimensional morphometric parameters (area, perimeter, roundness, and major and minor diameter) of root canals on different CBCT images using 2 segmentation methods (operator-dependent and Otsu's automatic methods), considering micro-CT images as the reference standard. The determination of the most suitable thresholding method for root canal evaluation in CBCT imaging would increase the clinical applicability of this type of assessment.

MATERIALS AND METHODS

Sample Selection

A preliminary micro-CT scan was performed using SkyScan 1174 (50 kV, 800 μ A; Bruker, Kontich, Belgium) to select 10 mandibular molars with mesial roots and two independent canals, and absence of pulp nodules and internal/external resorption. After scanning, the specimens were individually stored in plastic vials containing 1 mL of physiological saline and kept in an oven at 37 °C.

Micro-CT scan

The specimens were scanned on SkyScan model 1173 (Bruker), selecting 130 kV, 61 μ A, 360°, 0.4° of rotation step, and 0.25-mm bronze filter, resulting in a 90-minute scanning time for each tooth. At the end of the scan, the specimens were restored in an oven (37°C, 95% of relative humidity). After that, the images were reconstructed using NRecon software Version 1.6.6.0 (Bruker). Ring artifact

correction of 15 (scale 0–20), beam hardening correction of 30% (scale 0%–100%), smoothing of 3 (scale 0–10), and a histogram equalization from 0.0 (minimum value) to 0.002 (maximum value) were applied.

CBCT Scan

Each tooth was individually placed in a human mandible covered with Mix-D material (KU Leuven, Leuven, Belgium)¹⁵ to simulate hard and soft human tissues. Thereafter, they were scanned with the following CBCT devices: 3D Accuitomo 170 (J Morita Corporation, Kyoto, Japan), NewTom 5G (CEFLA, Imola, Italy), and NewTom VGi evo (CEFLA). High-resolution scanning parameters were selected according to each device (Table 1).

Image Registration

After the conversion of all images captured by micro-CT and CBCT imaging in Digital Imaging and Communications in Medicine/TIFF format, the viewing platform was used to check for the direction and position on the x-, y-, and z-axes. The CBCT images were superimposed with micro-CT images using MeVisLab (MeVis Medical Solutions AG, Bremen, Germany) software and saved as output flipped in Digital Imaging and Communications in Medicine/TIFF format.

Image Analysis

The registered images were converted to BMP files using 3DToCtan software (Bruker). The quantitative analysis of 2-dimensional parameters (area, perimeter, roundness, and major and minor diameters) were performed independently in CTAn v.1.18.4.0 software (Bruker) by 2 evaluators at a 7-day interval.

Images were assessed using 2 thresholding methods determined by the operator and Otsu's automatic methods. The first one was determined interactively, sorting segments that correspond to the dentin and to the root canal and obtaining the binary image.

Macrosequencing was then performed for correction of the segmented images (Fig. 1A–F). For testing the “automatic threshold,” the Otsu method available on CTAn was selected in which thresholding was automatic, and the remaining steps were performed in the same way as the segmentation performed by the operator.

Assessment of Accuracy

The accuracy of area, perimeter, roundness, and major and minor diameters was determined by calculating the absolute error (AE) and the mean absolute percentage error (MAPE), using as control the measurements of micro-CT images obtained by the operator through thresholding¹⁶. AE was calculated by the formula $AE = x_0 - x$ (x_0 denotes the mean value of the parameter and x is the mean for the control measurements). MAPE was calculated by the formula $MAPE = 100 \times AE/x$ with the results expressed in %. Positive AE or MAPE values indicate overestimated measurements, whereas negative values indicate underestimated ones, and values close to 0 denote good accuracy.

Statistical Analysis

Fleiss kappa was performed to check interrater and intrarater reliability. Quantitative data on area, perimeter, roundness, and major and minor diameters revealed normal distribution (Shapiro-Wilk test). Therefore, AE was estimated as the mean and standard deviation. Subsequently, 1-way analysis of variance was used for comparing thresholding methods applied by the operator and Otsu's automatic methods. To assess the performance of the CBCT devices, MAPE was calculated for each parameter using micro-CT measurements as reference values and thresholding determined by the operator.

RESULTS

Intraobserver and Interobserver Reliability

Fleiss kappa values were greater than 0.61 for all assessed parameters, showing substantial agreement. The highest levels of agreement were observed for micro-CT parameters ($P < .05$), and intraobserver reliability revealed values higher than 0.8, showing perfect agreement for the different CBCT machines.

Thresholding Method

After observing that the data were normally distributed ($P > .05$), AE was compared to assess the thresholding methods based on micro-CT images. Regarding the area, perimeter, and minor diameter (Table 2), there

TABLE 1 - Scanning Parameters for Micro-computed Tomographic (micro-CT) and Cone-beam Computed Tomographic Imaging

| | micro-CT SkyScan 1173 | 3D Accuitomo 170 | NewTom 5G | NewTom VGi evo |
|------------|--------------------------|----------------------|---------------------|---------------------|
| Current | 61 μ mA | 5 mA | 4.41 mA | 3 mA |
| Voltage | 130 kV(p) | 90 kV(p) | 110 kV(p) | 110 kV(p) |
| FOV | — | 4 × 4 | 6 × 6 | 5 × 5 |
| Voxel | 0.012 mm ³ | 0.08 mm ³ | 0.1 mm ³ | 0.1 mm ³ |
| Exposure | 1100 ms | 30.8 s | 7.3 s | 7.3 s |
| Filter | 0.2 mm brass | — | — | — |
| Rotation | 0.2 | — | — | — |
| Resolution | HR | HR | HR | HR |

FOV, field of view; HR, high resolution; kV(p), kilovolt peak.

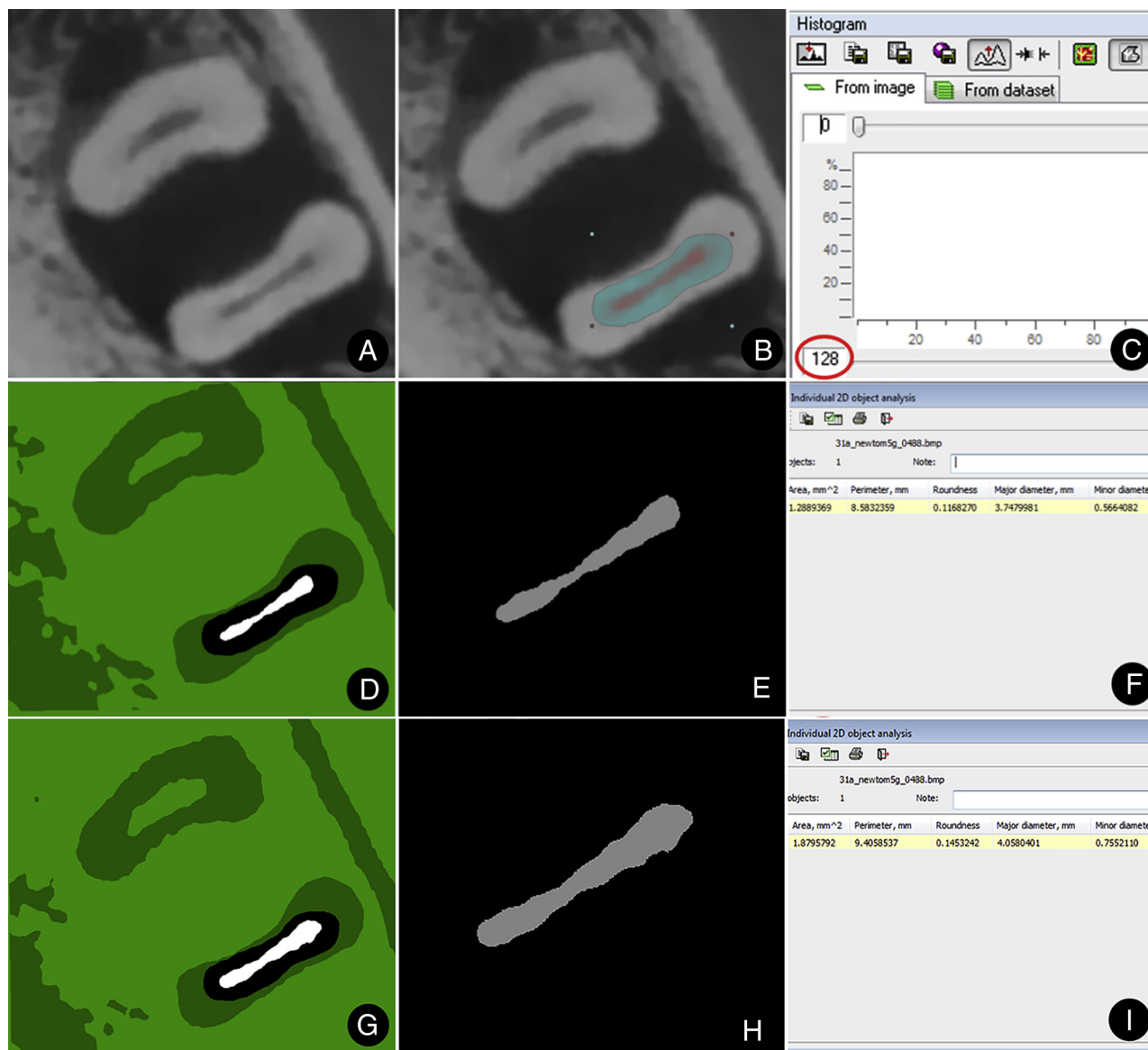


FIGURE 1 – The thresholding procedure determined by the operator and the automatic method using CTAn software. (A) An axial image of the NewTom VGi evo. (B) Selection of the area of interest. (C) Determination of the threshold by operator or Otsu's automatic method. (D) Visualization of the binarized image determined by operator. (E) Visualization of the binarized image determined by operator after postprocessing procedures. (F) Assessment of 2-dimensional morphometric parameters through the Individual Object Analysis (2-dimensional space) plug-in. (G) Visualization of the binarized image determined by Otsu's automatic method. (H) The binarized image of Otsu's automatic method after postprocessing procedures. (I) Assessment of 2-dimensional morphometric parameters through the Individual Object Analysis (2-dimensional space) plug-in. Note the quantitative difference between (E) operator's binary images and (H) Otsu's automatic method.

were differences between the values obtained by the 2 thresholding methods for all CBCT devices ($P < .0001$), with the lowest AE values observed for the method performed by the operator and no statistical difference between the measurements and different CBCT images ($P > .05$).

Regarding roundness and major diameter (Table 2), no difference was observed between the values for the thresholding method determined by the operator and Otsu's automatic methods and between CBCT images ($P > .05$).

Accuracy

Accuracy was assessed by MAPE based on the measurements obtained from micro-CT images. Note that the area and minor diameter had the highest MAPE values when Otsu's automatic method was used for all CBCT images, indicating overestimation of these parameters (Table 3). However, when perimeter was assessed using Otsu's automatic method, the values were underestimated (Table 3). On the other hand, when the thresholding performed by the operator was evaluated, the roundness

showed overestimated values (Table 3).

Interestingly, roundness and minor diameter, regardless of the thresholding method used, revealed overestimated values for all CBCT images (Table 3).

DISCUSSION

The thresholding method performed by the operator showed lower AE values for area, perimeter, and minor diameter when compared with Otsu's automatic method. This results can be suggested, since the operator-

TABLE 2 - Means and Standard deviations of Absolute Error (AE) for Each Cone-beam Computed Tomographic Scanner Obtained by Thresholding Methods (Determined by the Operator and Otsu's Automatic Method)

| Parameters | Evaluation Method | 3D Accuitomo 170 | NewTom 5G | NewTom VGi evO |
|----------------|-------------------------|---------------------------|---------------------------|---------------------------|
| Area | Performed by operator | 0.07 ± 0.39 ^A | 0.2 ± 0.37 ^A | 0.16 ± 0.43 ^A |
| | Otsu's automatic method | 1.27 ± 0.9 ^B | 0.94 ± 0.56 ^B | 0.85 ± 0.47 ^B |
| Perimeter | Performed by operator | 0.06 ± 0.3 ^A | 0.01 ± 0.26 ^A | -0.08 ± 0.18 ^A |
| | Otsu's automatic method | -0.38 ± 0.35 ^B | -0.17 ± 0.26 ^B | -0.3 ± 0.23 ^B |
| Roundness | Performed by operator | 1.42 ± 2.19 ^A | 0.68 ± 0.63 ^A | 1.02 ± 0.69 ^A |
| | Otsu's automatic method | 0.93 ± 0.74 ^A | 0.75 ± 0.59 ^A | 1.02 ± 0.74 ^A |
| Major diameter | Performed by operator | 0.12 ± 0.85 ^A | -0.09 ± 0.28 ^A | -0.21 ± 0.29 ^A |
| | Otsu's automatic method | 0.17 ± 0.37 ^A | 0.15 ± 0.52 ^A | -0.04 ± 0.36 ^A |
| Minor diameter | Performed by operator | 0.05 ± 0.3 ^A | 0.18 ± 0.3 ^B | 0.16 ± 0.29 ^A |
| | Otsu's automatic method | 0.64 ± 0.6 ^B | 0.57 ± 0.42 ^A | 0.59 ± 0.4 ^B |

3D, 3-dimensional.

Different uppercase letters in the column indicate statistical difference between the methods ($P < .05$).

dependent method allowed evaluators to determine the structure using specific tools (measurement tools) from the software combined with their knowledge of root canal morphology, and that the thresholding method directly interfered in the control and accuracy of the segmentation process. On the other hand, the values for Otsu's automatic thresholding may be related to the contrast resolution of each device because the delimitation and distinction between objects with different densities are automatic, taking into account the contrast and mean gray values^{13,14,16}.

As for roundness and major diameter values, there was no difference between the assessed methods, which may be explained by the larger linear dimensions of these parameters facilitating the identification and structural delineation of dentin and root canal by both methods.

Although studies on anatomy, biomechanical preparation, and filling of root canals using micro-CT mostly rely on thresholding methods determined by the operator^{17,18}, only Queiroz et al² compared both operator-dependent and automatic methods, concluding that there was no difference between methods for the assessment of 3-dimensional parameters,

whereas the present study revealed differences for 2-dimensional assessment. It should be noted that Lloyd et al¹⁷ and Stavileci et al¹⁸ did not describe the thresholding method.

When the accuracy of 2-dimensional parameters of the root canal was assessed, the parameters showed overestimation (roundness and minor diameter) or underestimation (perimeter) of CBCT (Accuitomo 170, NewTom 5G, and NewTom VGi evO) values, regardless of the thresholding method used. In this way, because area, roundness, perimeter, major diameter, and minor diameter are accurate measurements, slight variations in the thresholding limit could significantly increase MAPE. This may be attributed to the voxel sizes of CBCT images combined with differences in terms of voltage, current, and field of view when compared with better parameters used for micro-CT images¹⁹⁻²².

The MAPE for roundness and minor diameter revealed overestimated values, regardless of the assessed CBCT images. However, when area, perimeter, and major diameter were evaluated, the values underestimated by the thresholding method determined by the operator were more frequent. These differences between

underestimated and overestimated values can be associated with the resolution of CBCT imaging, when compared with micro-CT imaging, with a direct impact on sharpness and definition of small structures, especially regarding the determination of the borders of the assessed structures. In addition, it is suggested that the thresholding method determined by the operator allowed obtaining more reliable data because the expertise of operators in the manipulation of CBCT images directly influenced the delimitation of structures during the analysis^{19,20,22,23}.

The results obtained in the present study showed a tendency of overestimation of the 2-dimensional parameters of area, roundness, and major and minor diameters and an underestimation of the perimeter for the 3 CBCT machines evaluated (Accuitomo 170, NewTom 5G, and NewTom VGi evO). In this sense, these changes of the edges of structures assessed on CBCT images, because of the use of different segmentation methods, can hinder the qualitative and quantitative analysis as well as negatively influence clinical diagnosis in endodontics because they do not allow accurate determination of the original shape of the assessed structures^{9,24-29}.

TABLE 3 - Comparison of Percent Absolute Error (AE) by Thresholding Methods Performed by the Operator and Otsu's Automatic Method for Each Assessed Parameter

| | ACC | | N5G | | NEVO | |
|----------------|---------------------------|-----------------------------|---------------------------|-----------------------------|---------------------------|-------------------------|
| | Performed by operator (%) | Otsu's automatic method (%) | Performed by operator (%) | Otsu's automatic method (%) | Performed by operator (%) | Otsu's automatic method |
| Area | -19 | 128 | 20 | 95 | 16 | 85 |
| Perimeter | 7 | -38 | 2 | -17 | -9 | -30 |
| Roundness | 143 | 93 | 69 | 76 | 102 | 102 |
| Major diameter | 13 | 17 | -9 | 15 | -22 | -4 |
| Minor diameter | 6 | 65 | 19 | 57 | 16 | 59 |

ACC, Accuitomo; N5G, NewTom 5G; NEVO, NewTom VGi evO.

Indication of CBCT imaging for the assessment of area, perimeter, roundness, and major and minor diameters of root canals should be viewed with caution because these parameters had significant findings regarding overestimation and underestimation, mainly in the data obtained from images in which Otsu's automatic segmentation method was used. In the future, with breakthroughs in

research and technology, computed tomographic image reconstruction and analysis protocols are expected to overcome these limitations so that endodontists can safely indicate CBCT imaging, become aware of its limitations, and collect data from different reconstructions, improving diagnostic and prognostic predictability of endodontic treatment.

ACKNOWLEDGMENTS

We gratefully acknowledge financial support by the Coordination for the Improvement of Higher Education Personnel (CAPES, Brazil, nº 33002029032P4) and The São Paulo Research Foundation (FAPESP, Brazil, nº 2018/14450-1).

The authors deny any conflicts of interest related to this study.

REFERENCES

- Huang Y, Celikten B, De Faria Vasconcelos K, et al. Micro-CT and nano-CT analysis of filling quality of three different endodontic sealers. *Dentomaxillofac Radiol* 2017;46. 20170223.
- Queiroz PM, Rovaris K, Gaeta-Araujo H, et al. Influence of artifact reduction tools in micro-computed tomography images for endodontic research. *J Endod* 2017;43:2108–11.
- Lo Giudice R, Nicita F, Puleio F, et al. Accuracy of periapical radiography and CBCT in endodontic evaluation. *Int J Dent* 2018;2018. 2514243.
- Mamede-Neto I, Borges AH, Guedes OA, et al. Root canal transportation and centering ability of nickel-titanium rotary instruments in mandibular premolars assessed using cone-beam computed tomography. *Open Dent J* 2017;14:71–8.
- Dawood A, Patel S, Brown J. Cone beam CT in dental practice. *Br Dent J* 2009;207:23–9.
- Studebaker B, Hollender L, Aland L, et al. The incidence of second mesiobuccal canals located in maxillary molars with the aid of cone-beam computed tomography. *J Endod* 2018;44:565–70.
- Celikten B, Jacobs R, Vasconcelos KD, et al. Assessment of volumetric distortion artifact in filled root canals using different cone-beam computed tomographic devices. *J Endod* 2017;43:1517–21.
- Patel S, Dawood A, Ford TP, Whaites E. The potential applications of cone beam computed tomography in the management of endodontic problems. *Int Endod J* 2007;40:818–30.
- Schulze R, Heil U, Gross D, et al. Artefacts in CBCT: a review. *Dentomaxillofac Radiol* 2011;40:265–73.
- Versiani MA, Ordinola-Zapata R, Keles A, et al. Middle mesial canals in mandibular first molars: a micro-CT study in different populations. *Arch Oral Biol* 2016;61:130–7.
- Leoni GB, Versiani MA, Silva-Sousa YT, et al. Ex vivo evaluation of four final irrigation protocols on the removal of hard-tissue debris from the mesial root canal system of mandibular first molars. *Int Endod J* 2017;50:398–406.
- Sousa-Neto MD, Silva-Sousa YC, Mazzi-Chaves JF, et al. Root canal preparation using micro-computed tomography analysis: a literature review. *Braz Oral Res* 2018;32:20–43.
- Otsu N. A threshold selection method from grey-level histograms. *IEEE T Syst Man CY-S* 1979;9:62–6.
- Moreira AC, Appoloni CR, Mantovani IF, et al. Effects of manual threshold setting on image analysis results of a sandstone sample structural characterization by X-ray microtomography. *Appl Radiat Isot* 2012;70:937–41.
- Oenning AC, Salmon B, Vasconcelos KF, et al. DIMITRA paediatric skull phantoms: development of age-specific paediatric models for dentomaxillofacial radiology research. *Dentomaxillofac Radiol* 2018;47. 20170285.
- Damstra J, Fourie Z, Huddleston-Slater JJ, Ren Y. Accuracy of linear measurements from cone-beam computed tomography-derived surface models of different voxel sizes. *Am J Orthod Dentofacial Orthop* 2010;137:16.e1–6.
- Lloyd A, Uhles JP, Clement DJ, Garcia-Godoy F. Elimination of intracanal tissue and debris through a novel laser-activated system assessed using high-resolution micro-computed tomography: a pilot study. *J Endod* 2014;40:584–7.
- Stavileci M, Hoxha V, Gorduysus O, et al. Evaluation of root canal preparation using rotary system and hand instruments assessed by micro-computed tomography. *Med Sci Monit Basic Res* 2015;21:123–30.

19. Maret D, Peters OA, Galibourg A, et al. Comparison of the accuracy of 3-dimensional cone-beam computed tomography and micro-computed tomography reconstructions by using different voxel sizes. *J Endod* 2014;40:1321–6.
20. Nemtoi A, Czink C, Haba D, Gahleitner A. Cone beam CT: a current overview of devices. *Dentomaxillofac Radiol* 2013;42. 20120443.
21. Spin-Neto R, Gotfredsen E, Wenzel A. Impact of voxel size variation on CBCT-based diagnostic outcome in dentistry: a systematic review. *J Digit Imaging* 2013;26:813–20.
22. Michetti J, Basarab A, Tran M, et al. Cone-beam computed tomography contrast validation of an artificial periodontal phantom for use in endodontics. *Conf Proc IEEE Eng Med Biol Soc* 2015;2015:7905–8.
23. Pauwels R, Beinsberger J, Collaert B, et al. Effective dose range for dental cone beam computed tomography scanners. *Eur J Radiol* 2012;81:267–71.
24. Vasconcelos KF, Nicolielo LF, Nascimento MC, et al. Artefact expression associated with several cone-beam computed tomographic machines when imaging root filled teeth. *Int Endod J* 2015;48:994–1000.
25. Vasconcelos KF, Codari M, Queiroz PM, et al. The performance of metal artifact reduction algorithms in cone beam computed tomography images considering the effects of materials, metal positions, and fields of view. *Oral Surg Oral Med Oral Pathol Oral Radiol* 2018;127:71–6.
26. Codari M, Vasconcelos KD, Nicolielo LF, et al. Quantitative evaluation of metal artifacts using different CBCT devices, high-density materials and field of views. *Clin Oral Implants Res* 2017;28:1509–14.
27. Patel S, Durack C, Abella F, et al. Cone beam computed tomography in endodontics - a review. *Int Endod J* 2015;48:3–15.
28. Fox A, Basrani B, Kishen A, Lam EW. A novel method for characterizing beam hardening artifacts in cone-beam computed tomographic images. *J Endod* 2018;44:869–74.
29. Gaeta-Araujo H, De Souza GQ, Freitas DQ, De Oliveira-Santos C. Optimization of tube current in cone-beam computed tomography for the detection of vertical root fractures with different intracanal materials. *J Endod* 2017;43:1668–73.